Deformability Curve for K18 Steel

J. Pośpiech

(Submitted 29 December 1997; in revised form 7 June 1999)

Determination of plasticity of materials by the method of Kolmogorow is described. Variation of the stress factor for several plastic working processes is also described. Tests to plot the deformability curve (also referred to as reserve of plasticity curve) were selected and proved.

Keywords boundary deformability, metal forming, plasticity

Introduction

The problem of the best utilization of plasticity in plastic working processes of metals, at low resistance to deformation and maximum utilization of capacity of installations has gained great importance, especially in recent years. This can be attributed to a steady increase in tonnage of metals and alloys subjected to plastic working (metal forming) processes, as well as to the growing importance of plastic working in metal processing. It has also been demonstrated (Ref 1, 2) that a rather low utilization of plasticity in many metal working techniques can lead to application of annealings, which can decrease in number. This can result, in turn, in a prohibitive increase in production costs. In order to be able to work a metal plastically with the optimum utilization of its deformability, it is necessary to know the amount of permissible, permanent deformations necessary to obtain a desired shape of the final product. For this purpose, Kolmogorow (Ref 1, 2) introduced the concept of reserve of plasticity, by which a deformation from the yield point to the incipient fracture of metal is meant. A critical crack value, ψ_z, corresponds to this deformation range (being consistent macroscopically with the commencement of decohesion). Often, the definition of plasticity covers not only the ability of metal to undergo permanent deformation, but also a low resistance to deformation. Hence, the problem simplifies to determination of deformations, which would result in initiation of decohesion of metal or alloy, meaning that the reserve of plasticity of a given material is exhausted.

The goal of this study was to investigate the variation of the stress factor for selected plastic working processes and plot a curve of deformability, also called a curve of reserve of plasticity, or sometimes fracture or failure curve.

2. Description of Applied Theory of Failure of Materials

When determining the commencement of failure, the effect of stress on plasticity of metal at constant temperature and constant rate of deformation has to be determined because it is known that plasticity is not only a feature of a given material, but it is also a function of the stress state.

J. Pośpiech, Instytut Metalurgii Zelaza (Research Institute of Ferrous Metallurgy), ul. K. Miarki 12, 44-101 Gliwice, Poland.

The assumption of a criterion of initiation of failure is also important. There are two solutions possible. In the first concept the appearance of microcracks, as revealed macroscopically on polished sections, is considered as the beginning of failure. Takase (Ref 3) used a special etching reagent to reveal microcracks and presumably other minor imperfections. He detected only microcracks, without grain boundaries and slip lines. This etchant was composed of nitric acid, picric acid, ferrous chloride, and ethyl alcohol.

It seems, however, that such a conception of the problem merely complicates investigations and leads to an increase in expense and does not permit a greater accuracy of measurements because other measurements will further contain a great error, for example, the measurement of radius of curvature at the spot of fracture (with the use of workbench microscope). Therefore, the appearance of the first crack on the surface of specimen, as detected by the naked eye, was assumed to be a criterion of failure (the second possible solution); although in tensile testing of notched specimens, for example, this is consistent with the moment of specimen fracture.

In this study the theory of Kolmogorow (Ref 1, 2) was used as the most developed theory at the present time. Kolmogorow introduced the so-called coefficient of utilization of reserve of plasticity to evaluate the state of deformation in any manufacturing process. It is a scalar varying from 0 to 1. If this coefficient is zero, it means that metal did not undergo plastic deformation. If it reaches 1, it means that a first crack in the material has appeared; that is, a certain critical density of microcracks was reached by a given metal. This coefficient is given as a percent to denote the utilization of plasticity reserve of the material in a given working process. It is calculated from the following equation:

$$\psi_z = \int_0^{t_1} B(t)\,\frac{\gamma_i\,dt}{g_{iz}[k(t)]} \qquad \text{(Eq 1)}$$

where:

$$g_{iz} = \int_0^{t_1} \gamma_i(t)\,dt \qquad \text{(Eq 2)}$$

$$\gamma_i = +\sqrt{\tfrac{2}{3}[(\varepsilon_x - \varepsilon_y)^2 + (\varepsilon_y - \varepsilon_z)^2 + (\varepsilon_z - \varepsilon_x)^2] + \gamma_{xy}^2 + \gamma_{yz}^2 + \gamma_{zx}^2} \qquad \text{(Eq 3)}$$

$$k = \frac{\sigma_m}{\tau_i} \qquad \text{(Eq 4)}$$

where:

g_{iz} is the effective strain at the moment of fracture, in distortion energy hypothesis.

t is time.

ε_x, ε_y, ε_z, γ_{xy}, γ_{yz}, and γ_{zx} are components of tensor of deformation velocity.

ψ_z is the coefficient of utilization of reserve of plasticity.

$B(t)$ is a function describing the nonmonotonic nature of the process.

γ_i is the intensity of deformation velocity in distortion energy hypothesis.

k is the state of stress factor.

σ_m is the mean stress.

τ_i is the intensity of shearing stresses.

However, in order to make use of Eq 1, the relationship $g_{iz} = f[k(t)]$ must be known. If this function is represented graphically, a reserve of plasticity curve, also known as a deformability curve, can be obtained. This curve is plotted for mechanical tests, for which k varies within a range. Of importance is, therefore, the determination of range of variation of k for plastic working processes to obtain in testing stress states similar to those occurring in technological processes.

Numerous investigations have been made in this field at the Research Institute of Ferrous Metallurgy in Gliwice, Poland (Ref 4-9), including an investigation of the influence of nonhomogeneity of materials on their deformability (Ref 10, 11). An investigation was also carried out to find one test to determine deformability of steels in different states of stress and strain (Ref 8, 9) and to standardize specimens. An effort was made to find practical solutions to the theory of boundary deformability (Ref 7). An interest in these problems has returned in Poland because of new investments in metallurgy (Ref 12, 13).

Wide investigations were carried out by researchers from the University of Glasgow (Ref 14-22). They investigated stress and strain concentrations around a rigid inclusion in a plastically deformed matrix using continuum mechanics. Void nucleation, growth, and coalescence were also studied. Deformability curves for a few materials in the long and short transverse directions were determined. Axisymmetrical and plane strain notch tensile specimens were used. An equation of a deformability curve was derived theoretically (Ref 14) by improving criterion created by Rice and Tracey (Ref 23). However, there is no practical use of this knowledge for such processes as tube drawing or rolling.

El-Magd (Ref 24) published curves of deformability for iron and austenitic steel determined under quasi-static and dynamic loading. Notched specimens in a tensile test were used. The target of this investigation was to study the effect of dynamic loading on boundary deformability.

So-called failure curves are also presented in Ref 25 and 26. These curves were determined from experiments and by a special procedure using a yield equation. Smooth and notched tensile specimens were used to determine failure curves.

A review of different models used for determination of boundary deformability is presented by Thomason (Ref 27). Curves of deformability are also described.

An investigation of the influence of principal stress, σ_2, where $\sigma_1 > \sigma_2 > \sigma_3$ on a deformability curve is presented by Vater and Lienhart (Ref 28). Deformability is higher if the difference between σ_2 and σ_3 (the smallest principal stress) is smaller and the stress factor is the same (Ref 28).

A deformability curve (as an equation) was derived theoretically by Schiller (Ref 29), Rice and Tracey (Ref 23), and Hancock and Makenzie (Ref 14).

3. Determination of Stress Factor for Typical Plastic Working Processes

In this section variation ranges of stress factors for selected plastic working processes have been calculated. Independent variables were established from practice (Ref 4).

3.1 Sinking of Tubes

The stress factor state calculated by Kolmogorow (Ref 1, 2) can be obtained from the formula:

$$k = \frac{\sigma_m}{\tau_i} = \frac{1 - 3z^3}{\sqrt{3}\sqrt{1 + 3z^6}} \qquad \text{(Eq 5)}$$

$$z = \frac{d_1}{d_0}$$

where d_1 is the outside diameter of tube after pass and d_0 is the outside diameter of tube before pass.

The stress factor state has been calculated for the most popular case of tube drawing, for which coefficient of friction $f = 0.1$ and the half die angle $\alpha = 12°$. Because z varies theoretically from 0 to 1 and practically from 0.78 to 1, the stress factor varies as (Ref 4):

$$-0.577 \le k \le 0.577 \qquad \text{for } 0 \le z \le 1$$

$$-0.577 \le k \le 0.014 \qquad \text{for } 0.7 \le z \le 1$$

3.2 Drawing of Tubes on Stationary Mandrel

When calculating the stress factor for this working process, the deformation region is divided in two zones. For the first zone, a reduction zone, the stress factor is calculated in the same way as for drawing tubes without a mandrel. For the second zone, a necking zone, the factor, k, is calculated from the following formula:

$$k = 2\left(1 - 3\sqrt{\frac{d_1}{d_0}}\right)\frac{s_1}{s_0} + 3 \qquad \text{(Eq 6)}$$

where d_1 is the outside diameter of the tube at the entry into the necking zone, d_0 is the outside diameter of tube before pass, s_1 is the tube wall thickness after pass, and s_0 is the tube wall thickness at the entry into the necking zone.

In that deformation zone the stress factor varies, as shown in the following equations (Ref 4). For the theoretical range of variation d_1/d_0 and s_1/s_0:

$$0 < \frac{d_1}{d_0} < 1$$

and

$$0 < \frac{s_1}{s_0} < 1$$

the factor k varies within $-1 < k < 5$. For variation range encountered in practice d_1/d_0 and s_1/s_0:

$$0.7 < \frac{d_1}{d_0} < 1$$

and

$$0.33 < \frac{s_1}{s_0} < 1$$

the stress factor varies within $-1 < k < 2.1$.

The total stress factor has to be calculated by taking into account the stress in both the deformation zones. However, because k assumes negative values in the first deformation zone, only the stress factor in the second deformation zone can be adopted to evaluate the drawing process. Negative values of k in the first deformation zone diminish the total value of the stress factor, which increases the security of the drawing process.

3.3 Drawing of Tubes on Floating Mandrel

In this article, calculations have been based on data given by Kolmogorow (Ref 1, 2). The stress factor that has been computed for the most frequent drawing conditions, that is, half die angle $\alpha = 12°$ and coefficient of friction, $f = 0.1$. Similarly, as in the previous case, the deformation region was divided in two zones. For the first zone, called the reduction zone, the stress factor was calculated in the same way as for tube sinking. For the second zone, the necking zone, the factor, k, is computed from the formula:

$$k = 5 - 6\sqrt{\frac{d_1}{d_0}} + 2\ln\frac{s_0}{s_1} \qquad \text{(Eq 7)}$$

In that deformation zone the stress factor varies as shown in the following equations. For the theoretical range of variation:

$$0 < \frac{d_1}{d_0} < 1$$

and

$$0 < \frac{s_1}{s_0} < 1$$

the factor, k, varies within $-1 < k < 9.6$. For the variation range met in practice:

$$0.65 < \frac{d_1}{d_0} < 1$$

and

$$0.5 < \frac{s_1}{s_0} < 1$$

the factor, k, changes within $-1 \le k \le 1.27$.

In the case of drawing tubes on a floating mandrel, the total stress factor has to be calculated by taking into account the stress in both deformation zones. However, because k assumes negative values in the first deformation zone, only the factor, k, for the second deformation zone can be employed to evaluate the deformation process, which provides a greater security in drawing. From a comparison of k for both stationary and floating mandrel drawing processes, it is well known that in a floating mandrel drawing, a more favorable stress occurs. This means that by taking similar reductions, the reserve of plasticity in a floating mandrel drawing will be exhausted more slowly.

3.4 Drawing of Round, Full-Section Bars

Calculations of the stress factor have been made on the basis of publication (Ref 30). In the drawn bar, two deformation zones with different stress distributions can be distinguished. In the first zone where the material comes in contact with the die hole surface, a cylindrical stress state exists that is determined by the tensile stress, σ_1, and compressive stresses, σ_2 and σ_3, of equal value. In the second, middle zone, on the contrary, there is tensile stress. Because the material will fail in the second deformation zone, only the stress factor for that zone has been calculated. It is described by the following equation:

$$k = 0.577 - 0.577e^{-\gamma} \cdot \frac{q}{1-q} \qquad \text{(Eq 8)}$$

where according to Ref 30:

$$\gamma = \frac{\mu + tg\,\alpha}{(1 - \mu\ tg\,\alpha)\ tg\,\alpha}$$

$$q = 1 - \frac{S_1}{S_0}$$

where μ is the coefficient of friction, α is the angle of die reduction cone, S_1 is the cross-sectional area of bar after drawing, and S_2 is the cross-sectional area of bar before drawing.

To determine the range of variation of the stress factor, an assumption was made consistent with practice that parameters μ, α, and q vary within the following limits (Ref 4): $\mu = 0.08$, $\alpha = 6°$ to 16°, and $q = 0.05$ to 0.5.

Calculations have shown that the stress factor in the drawing process varies within $0.037 \le k \le 0.4794$.

3.5 Drawing with Back Tension

In this section the drawing of round-section products is discussed. The stress distribution was determined on the basis of data contained in literature (Ref 31-33). When calculating the stress factor, an assumption was made that at the critical spot there exists one axial tensile stress. On making necessary transformations the following equation is obtained:

$$k = 0.577 \frac{a+1}{a \cos^2 \frac{\alpha + \rho}{2}} (q)^{a/2} + 0.577 \frac{\sigma_q}{k_{fsr}} (1-q)^{a/2} \qquad \text{(Eq 9)}$$

where:

$$a = (1 + f \operatorname{ctg} \alpha') \cos^2 \rho - 1$$

$$q = 1 - \left(\frac{D_z}{D_H}\right)^2$$

$$\operatorname{ctg} \alpha' = \frac{1 + 2m \frac{\sqrt{1-q}}{1-\sqrt{1-q}} \operatorname{tg} \alpha}{\operatorname{tg} \alpha}$$

where:

α is the angle of die reduction cone.

ρ is the arc tg f, f-coefficient of friction.

σ_q is the back tension stress (always greater than elastic limit of the material).

q is the relative reduction of cross-sectional area of drawn bar.

D_H is the diameter of bar before drawing.

D_z is the diameter of bar leaving the reduction zone prior to entry to die parallel.

m is the ratio of parallel zone length to diameter of bar passing through it: $m = l_k/D_k$.

To calculate the variation range for the stress factor, the following range of variations for parameters in Eq 9 has been assumed:

- m varies from 0.2 to 1.5.
- α varies from 6 to 16°.
- q varies from 0.05 to 0.5.
- σ_q/K_{fsr} varies from 0.14 to 0.56.
- $f = 0.08$

hence, $\rho = 4°34'$.

The range of variation for the quotient σ_q/K_{fsr} was assumed for orientation only. It is difficult to determine it exactly because both these values depend on material and amount of deformation not permitting a more exact calculation. Therefore calculations have been made for a case when $\sigma_q = 0$, that is, for a case of simple drawing. The range of variation of the stress factor, as obtained from these calculations, is $0.00000001 < k < 2.52$. The accuracy with which this factor has been calculated is astonishing. This was done to emphasize the difference between the stress in the drawing process ($k = 0.00000001$) and that occurring in torsion tests on cylindrical specimens ($k = 0$).

Further, calculations have been carried out for the case when $\sigma_q \neq 0$. These calculations have shown that in drawing with back tension the stress factor varies within $0.0625 < k < 2.815$.

3.6 Cold Pilger Rolling of Tubes

The deformation and stress states have been determined based on distortion of a grid cut on the surface of the tested tubes (Ref 1, 2). It should be remembered that the stress for this process is difficult to define mathematically because it changes from a three-axial compression to two-axial tension, depending on the position of the deformed zone relative to the rolls. Investigations carried out by Kolmogorow have shown that the stress factor within the tube varies from –2.8 to +0.8 depending on the deformed zone. Kolmogorow (Ref 1, 2) also investigated the influence of elongation, angle of torsion, and pitch (advance) on the stress factor.

It appeared that variations of elongation and pitch have a negligible effect on the stress factor. The angle of torsion effect was greater, but it did not cause major changes in the stress.

3.7 Hot Rolling

To calculate the stress, the method given by Geleji (cited in Ref 34, 35) was used. This method applies, in principle, to rectangular sections, but it can also be used, with a lesser accuracy, to determine the stress distribution in other regular passes. In making necessary transformations, the stress factor can be determined from the following equation:

$$k = -1.155 \left[1 + c \frac{l_d}{h_m} a(0.86 - 0.025 v_r) \sqrt[4]{v_r} \cdot (1.05 - 0.0005t) \right] \qquad \text{(Eq 10)}$$

where l_d is the projection of arc of contact:

$$l_d = \sqrt{R \Delta h}$$

h_m is the mean height of rolled stock:

$$h_m = \frac{h_1 + h_2}{2}$$

v_r is the peripheral speed of rolls, m/s.

t is the temperature of rolled stock, °C.

a is the factor depending on roll material (a = 1 for cast iron and rough steel rolls, a = 0.8 for chilled rolls and smooth steel rolls, and a = 0.55 for ground steel rolls).

c is the factor determined from the following equations if:

$$0.25 \le \frac{l_d}{h_m} \le 1$$

then:

$$c_1 = 17\left(\frac{l_d}{h_m}\right)^2 - 29.85\,\frac{l_d}{h_m} + 18.3 \qquad \text{(Eq 11)}$$

if:

$$1 \le \frac{l_d}{h_m} \le 3$$

then:

$$c_2 = 0.8\left(\frac{l_d}{h_m}\right)^2 - 4.9\,\frac{l_d}{h_m} + 9.6 \qquad \text{(Eq 12)}$$

if:

$$3 \le \frac{l_d}{h_m} \le 13$$

then:

$$c_3 = 0.013\left(\frac{l_d}{h_m}\right)^2 - 0.29\,\frac{l_d}{h_m} + 2.86 \qquad \text{(Eq 13)}$$

In the hot-rolling process the variables from Eq 10 change within the following limits: $0.25 \le l_d/h_m \le 13$, $2 \le v_r \le 22$, and $900 \le t \le 1200$. The factor, a, assumes three values: 1, 0.8, or 0.55.

Calculations have shown that the stress factor in hot rolling varies within $-14.3 \le k \le -1.703$.

3.8 Calculations of Stress Factor and Variation Range in Hot Rolling When the Effect of Additional Friction during Rolling in Passes is Taken into Account

Wusatowski and Ludyga (Ref 34, 35) found that rolling in box passes increases the rolling load, the mean resistance to deformation, and the rolling torque. Of course, components of the stress tensor increase, too. They gave consistent coefficients for these increases. In calculations, the stress factor can be determined from the equation:

$$k = -1.155\,a_1\left[1 + c\,\frac{l_d}{h_m}\,a(0.86 - 0.025 v_r)\,\sqrt[4]{v_r}\cdot(1.05 - 0.0005\,t)\right] \qquad \text{(Eq 14)}$$

where a_1 is a factor varying within $1.05 \le a_1 \le 1.85$. The remaining notations are the same as given in the previous section. In this process the variables on the right side of Eq 14 change within the following limits:

$$0.25 \le \frac{l_d}{h_m} \le 13 \qquad 2 \le v_r \le 22$$

$$900 \le t \le 1100 \qquad 1.05 \le a_1 \le 1.85$$

and the factor a assumes three values: 1, 0.8, or 0.55. The calculations have shown that the stress factor assumes values within $-26.45 \le k \le -1.857$.

3.9 Cold Rolling

Use was made of the theory of Nadai (Ref 36) in which an assumption is made that between the rolled stock and the rolls, a slip occurs with fluid friction. Such an assumption is, of course, a simplification, but there are cases in practice for which it can be made. Such a case exists in cold rolling where abundant lubrication of well-ground rolls and high rolling speeds (5 to 20 m/s) are applied. Under such conditions the fine particles of the contacting rolls are subjected to friction, the nature of which is similar to that of fluid friction. In this rolling process the stress in metal is three-axial compressive. The stress factor for the cold rolling process can be described by the equation:

$$k = 1.993\left[\xi_1 + \ln(1+z)^2 + \frac{A\tau}{2}\left(\frac{z}{1+z^2} - B\,\text{arc}\,tg\,z\right)\right] - 1 \qquad \text{(Eq 15)}$$

Variables ξ_1, z, A, and B in this equation are obtained from:

$$A = \frac{2l}{\sqrt{h_1\,\Delta h}}$$

$$B = \frac{(2k'/A\tau)[\xi_1 - \xi_0 + \ln(1+z_0^2)] + \left[z_0/(1+z_0^2)\right]}{\text{arc}\,tg\,z_0}$$

$$z_0 = \sqrt{\frac{\Delta h}{h_1}}$$

$$z = \frac{1}{l_d}\sqrt{\frac{\Delta h}{h_1}} \cdot x$$

$$\xi_1 = 1 - \frac{\sigma_n}{k'} \qquad \xi_0 = 1 - \frac{\sigma_i}{k'}$$

$$k' = 1.15\, k_f$$

where:

k_f is the yield stress.

τ is the unit frictional force at the slip velocity equal to the metal speed at the exit from rolls.

l_d is the projection of arc of contact: $l_d = \sqrt{R\Delta h}$

R is the roll radius.

h_0 and h_1 are the height of rolled stock before and after the pass, respectively.

Δh is the absolute draught.

σ_n and σ_i are the respective forward and back tension stresses.

x is a current variable measured along the rolling line, it varies within: $0 < x < \sqrt{R\Delta h}$

The following variation ranges for variables in Eq 15 have been adopted from Ref 36 and 37:

- $h_1 = 0.1$ mm
- $\Delta h/h_1$ varies from 0 to 1.
- $D = 2R$ varies from 40 to 550 mm.
- $\xi_1 = \xi_0$ varies from 0.31 to 0.827 or $\xi_1 = \xi_0 = 1$.

Calculation of the variation range for the stress factor occurring in this rolling process was rather difficult because Eq 15 contains a current variable, x. Therefore, by substituting the parameters characterizing the rolling process into Eq 15 and 16, extremes of the function $k = f(x)$ were found. Hence, the results of calculations must be regarded as approximations. The calculations have shown that the stress factor varies within $-190.8 < k < -1$. This result is interesting, but it should be remembered that calculations are approximative and refer to extreme cases, rather seldom met in practice.

The stress state in the rolling process is also assumed to be three-axial compression, although it is known that fracture will occur on the edge of the rolled strip where tensile stresses occur. However, the lack of a formula describing the stress state at the place of fracture did not allow for making a more precise analysis of this problem.

Further, the method of determining the deformability curve is given from results obtained in mechanical tests. By using this curve, it can be determined when the reserve of plasticity will be exhausted under given conditions of a working process.

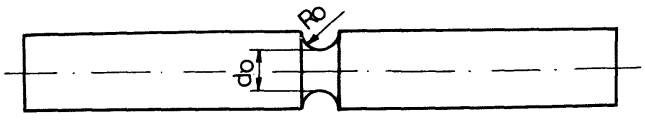

Fig. 1 Cylindrical specimen with a notch. (a) d_0 is diameter of specimen at the spot of turned notch. (b) R_0 is the radius of curvature of the specimen generating line.

4. Determination of Deformability Curve for K18 Steel

4.1 Description of Stress State and Strain State in Tensile and Upending Tests

In determining the deformability curve (also called the curve of reserve of plasticity) the problem of selection of suitable mechanical tests is important. The most appropriate method would be a test in which the entire curve could be obtained because (Ref 4) (a) it is known in engineering that the most comparative results are those obtained under the same conditions (e.g., temperature, testing apparatus, environment), and (b) the stress state and deformation state (strain) in a given test are described differently by various authors. This complicates the situation when several tests are applied because it is difficult to choose valid equations for several tests. A further criterion for selection of tests is the facility to determine the commencement of failure.

The fourth criterion consists in obtaining a constant value of stress factor state and constant strain rate (deformation velocity), as well as in maintaining a monotonic deformation progress under conditions of the test.

The final criteria for selection of a test are the costs involved, the facility used for the test procedure, and reproducibility of results. In these investigations the two tests were carried out, the tensile test on cylindrical specimens with turned ring groove and the compression test on cylindrical specimens. These tests are widely used, are relatively inexpensive, and provide reproducible results.

The tensile test carried out on specimen shown in Fig. 1 obtained several points of the deformability curve by changing the d/R ratio. This test does not allow determination of the start of failure (appearance of the first microcrack revealed by the naked eye) because the fracture occurs suddenly and covers the whole cross section of the specimen. This is precise in macroscopic respect, only, because the first cracks appear in the specimen axis. They are, however, not visible for the observer following the progress of failure from the outside. The unquestionable advantage of the tensile test is the fact that the plastic deformation at the place of failure progresses monotonically. To determine the stress factor state and the effective strain, the formula given by Dawidenkow and Spiridonowa (cited in Ref 1 and 2) were used.

At the fracture location in the specimen neck, the stress state is three-axial tensile. The stress factor state determined from Eq 4 takes the form (based on the formula derived by Dawidenkow and Spiridonowa):

$$k = 0.577 + 0.433\,\frac{d_1}{R_1} \qquad \text{(Eq 17)}$$

The effective strain at the moment of fracture will be:

$$g_{iz} = 2\sqrt{3}\,\ln\frac{d_0}{d_1} \qquad \text{(Eq 18)}$$

where d_0 and d_1 are the diameter of specimen at the spot of fracture before and after breakage, respectively, and R_1 is the radius of curvature of the specimen generating line at the spot of fracture after breakage.

The upending test on cylindrical specimens with orthogonal square mesh grids cut on the side surface of the specimen is an important test in that it allows that part of the deformability curve, which is essential from practical point of view, to be obtained. The variable factors in this test are the friction (dependent on the variety of lubricants used) and the varying ratio of specimen height to specimen diameter prior to deformation. In this test the stress factor varies from $k = -0.58$ (compression without barreling) to positive values depending on degree of barreling.

The advantage of this test consists in providing the possibility to determine the commencement of fracture. The fracture will occur on the side surface of specimen, amid the height of specimen. The major disadvantage of the upending test is nonmonotonic progression of plastic deformation at the fracture location. This considerably hinders the mathematical description of deformation. However, the so-called simple compression, that is, compression without barreling, is possible (to date in theory, only). In such a case the deformation process would proceed monotonically and the stress factor would be constant, $k = -0.58$. Such a case is practically not feasible. The stress factor and the effective strain were calculated on the basis of Ref 38.

4.2 Experimental Results

Material Tested. Investigations have been carried out on K18 steel with the following analysis: 0.19% C, 0.98% Mn, 0.27% Si, 0.028% P, 0.023% S, 0.13% Cr, 0.08% Ni, and 0.08% Cu. The steel was reheated in a furnace and then forged at 1180 °C to bars of 18 mm diameter. After forging, the bars were air cooled. From this test material, standard test specimens were prepared by turning and polishing for mechanical tests. Tensile test specimens with the turned notch were turned and additionally ground at the notch location.

Specimens for the upending test were turned. A part had a grid on the surface, obtained by turning and milling. The depth of the grid was 0.2 mm (Ref 4).

Static Tensile Test. This test was carried out on a 10 ton tensile testing machine manufactured by Amsler. The dynamometer was set at a load of 5 tons. Seven specimens were tested. The form and dimensions of these specimens were specified in standard specification. The purpose of this test was to determine mechanical properties of steel used for investigations. The results of this test are mean, $d_0 = 7.99$ mm; mean yield point, $R_e = 40.35$ kg/mm^2; mean tensile strength, $R_m = 54.87$ kg/mm^2; mean elongation, $A_5 = 30.7\%$; mean elongation, $A_{10} = 22.45\%$; and mean contraction (necking down), $Z = 68.52\%$.

Tensile Test on Notched Specimens. For this test seven specimens with initial dimensions, $d_0 = 10$ mm and $R_0 = 2.5$ mm, and seven specimens with notch dimensions, $d_0 = 4$ mm and $R_0 = 8$ mm, were used. Such dimensions were adopted. In practice, there were some deviations. The lengths and outside diameters of the applied specimens were $D_0 = 15$ mm and $l_0 = 250$ mm and $D_0 = 14$ mm and $l_0 = 240$ mm.

The tensile test was carried out on 10 tonf (9.97 kN) tensile testing machine manufactured by Amsler. During the test the advance of the jaw was 1 mm/min. The radius of curvature was measured by the method described in Ref 39 under the workbench microscope. Table 1 lists the test results.

Upsetting Test on Cylindrical Specimens. This test was carried out on a press to obtain the flow rate approximately equal to that obtained in tensile testing. Because the press was controlled by a lever, this flow rate could not be established accurately. The ratio of h_d/d_0 was 1 for all the specimens. Specimens with a grid cut on the side surface and specimens without the grid were both tested.

The upending tests were carried out under the following lubrication conditions.

- Without any lubricant
- With the use of a paste composed of drawing practice powder and palm oil, applied on both the end surfaces of specimen
- With the use of molybdenum disulfide powder, which was rubbed into that end surface of specimen that came in contact with the movable part of the press
- With the use of molybdenum disulfide powder rubbed into both end surfaces of the specimen

Table 1 Calculation of effective strain and stress factors in tensile testing on notched specimens

Specimen No.	d_0, mm	d_1, mm	R_0, mm	R_1, mm	k	g_{iz}	k_{av}	$(k - k_{av})/k_{av} \cdot 100\%$, %	$[(k - k_{av})/k_{av} \cdot 100\%]_{av}$, %	g_{izav}	$(g_{iz} - g_{izav})/g_{izav} \cdot 100\%$, %	$[(g_{iz} - g_{izav})/g_{izav} \cdot 100\%]_{av, \%}$
1	10.0	7.0	2.554	2.308	1.891	0.24	1.887	0.21	1.91	0.229	4.81	3.80
2	10.0	6.9	2.539	2.370	1.841	0.248	…	2.42	…	…	8.30	…
3	10.1	7.2	2.537	2.306	1.920	0.226	…	2.2	…	…	1.31	…
4	10.0	7.2	2.541	2.41	1.871	0.22	…	0.85	…	…	3.93	…
5	10.0	7.3	2.545	2.37	1.91	0.210	…	1.21	…	…	7.86	…
6	10.0	7.1	2.551	2.238	1.952	0.229	…	3.44	…	…	0.00	…
7	10.3	7.3	2.545	2.54	1.82	0.23	…	3.1	…	…	0.43	…
1	4.0	2.9	7.81	1.13	1.689	0.215	1.464	15.38	7.20	0.325	33.85	17.38
2	4.0	2.4	7.77	1.352	1.344	0.344	…	8.20	…	…	5.84	…
3	4.0	2.8	7.702	1.197	1.590	0.238	…	8.60	…	…	26.75	…
4	4.0	2.3	7.832	1.3	1.342	0.37	…	8.33	…	…	13.82	…
5	4.0	2.3	7.755	1.148	1.446	0.37	…	1.22	…	…	13.82	…
6	4.0	2.3	7.74	1.279	1.356	0.37	…	7.36	…	…	13.82	…
7	4.0	2.3	7.811	1.098	1.484	0.37	…	1.36	…	…	13.82	…

Table 2 Results of upending test without lubrication

Spec. No.	Spec. type	h_0, mm	h_1, mm	d_0, mm	d_1, mm	h_0/d_0	m	g_{iz}	k	g_{izav}	k_{av}	$(g_{iz} - g_{izav})/g_{izav} \cdot 100\%$, %	$[(g_{iz} - g_{izav})/g_{izav} \cdot 100\%]_{av}$, %	$(k - k_{av})/k_{av} \cdot 100\%$, %	$[(k - k_{av})/k_{av} \cdot 100\%]_{av}$, %
1	4s	14.9	4.1	14.9	24.4	1	0.0914	1.259	0.343	1.1995	0.385	4.96	6.76	10.9	8.96
2	5s	15.0	4.6	14.9	27.6	1.006	0.081	1.23	0.391	…	…	2.54	…	1.56	…
3	1s	14.9	5.1	14.9	24.2	1	0.0654	1.13	0.438	…	…	5.8	…	13.78	…
4	4s	…	…	…	…	…	0.0792	1.1136	0.362	…	…	7.16	…	5.98	
5	5s	…	…	…	…	…	0.0792	1.345	0.434	…	…	12.12	…	12.7	…
6	1s	…	…	…	…	…	0.0792	1.115	0.35	…	…	7.05	…	9.1	…
7	3b	14.7	5.8	14.9	24.2	0.986	0.0792	1.115	0.35	…	…	7.05	…	9.1	…
8	4b	15.1	4.9	14.9	26.7	1.013	0.0792	1.289	0.418	…	…	7.46	…	8.58	…

Table 3 Results of upending test on specimens with molybdenum disulfide applied on one end surface of specimen (in contact with movable part of press)

Spec. No.	Spec. type	h_0, mm	h_1, mm	d_0, mm	d_1, mm	h_0/d_0	m	g_{iz}	k	g_{izav}	k_{av}	$(g_{iz} - g_{izav})/g_{izav} \cdot 100\%$, %	$[(g_{iz} - g_{izav})/g_{izav} \cdot 100\%]_{av}$, %	$(k - k_{av})/k_{av} \cdot 100\%$, %	$[(k - k_{av})/k_{av} \cdot 100\%]_{av}$, %
1	6s	15.0	4.0	14.9	29.35	1.006	0.1216	1.481	0.2695	1.455	0.252	1.78	4.94	6.95	18.99
2	6s	…	…	…	…	…	0.1183	1.587	0.3245	…	…	9.08	…	28.55	…
3	5b	14.9	5.7	14.9	24.9	1	0.1183	1.318	0.132	…	…	9.41	…	47.6	…
4	6b	15.0	4.8	14.9	26.7	1.006	0.1183	1.412	0.2535	…	…	2.95	…	0.59	…
5	7b	15.0	4.7	14.9	27.6	1.006	0.1183	1.477	0.2805	…	…	1.51	…	11.3	…

Source: Ref 4

Table 4 Results of upending test made with molybdenum disulfide applied on both end surfaces of specimen

Spec. No.	Spec. type	h_0, mm	h_1, mm	d_0, mm	d_1, mm	h_0/d_0	m	g_{iz}	k	g_{izav}	k_{av}	$(g_{iz} - g_{izav})/g_{izav} \cdot 100\%$, %	$[(g_{iz} - g_{izav})/g_{izav} \cdot 100\%]_{av}$, %	$(k - k_{av})/k_{av} \cdot 100\%$, %	$[(k - k_{av})/k_{av} \cdot 100\%]_{av}$, %
1	0s	15.0	3.3	15.0	31.8	1.0	0.131	1.662	0.295	1.509	0.3034	11.3	6.74	2.77	10.4
2	1s	15.0	4.3	15.0	28.8	1.0	0.1074	1.462	0.3344	…	…	3.12	…	10.2	…
3	7s	15.1	4.3	15.0	28.8	1.0	0.12	1.446	0.26	…	…	4.17	…	14.3	…
4	8s	15.0	4.7	15.0	27.3	1.0	0.1073	1.295	0.257	…	…	14.2	…	15.3	…
5	0s	…	…	…	…	…	0.1164	1.711	0.374	…	…	13.4	…	23.2	…
6	1s	…	…	…	…	…	0.1164	1.532	0.3162	…	…	1.52	…	4.22	…
7	7s	…	…	…	…	…	0.1164	1.532	0.3162	…	…	1.52	…	4.22	…
8	8s	…	…	…	…	…	0.1164	1.438	0.275	…	…	4.7	…	9.36	…

Source: Ref 4

Table 5 Results of upending test made on specimens lubricated with a paste composed of drawing powder and palm oil

Spec. No.	Spec. type	h_0, mm	h_1, mm	d_0, mm	d_1, mm	h_0/d_0	m	g_{iz}	k	g_{izav}	k_{av}	$(g_{iz} - g_{izav})/g_{izav} \cdot 100\%$, %	$[(g_{iz} - g_{izav})/g_{izav} \cdot 100\%]_{av}$, %	$(k - k_{av})/k_{av} \cdot 100\%$, %	$[(k - k_{av})/k_{av} \cdot 100\%]_{av}$, %
1	2s	15.0	3.1	15.0	34.0	1.0	0.1469	1.73	0.2447	1.627	0.1873	6.34	7.15	30.5	39.5
2	3s	15.0	4.1	15.0	29.3	1.0	0.2098	1.704	–0.0703	…	…	4.74	…	137.1	…
3	4s	15.1	4.1	15.0	29.3	1.006	0.1371	1.581	0.2279	…	…	2.82	…	21.6	…
4	5s	15.1	4.8	15.0	27.0	1.006	0.1372	1.409	0.1345	…	…	13.4	…	28.1	…
5	6s	15.0	4.3	15.0	29.2	1.0	0.113	1.428	0.2917	…	…	12.2	…	55.6	…
6	2s	…	…	…	…	…	0.1488	1.930	0.3075	…	…	18.6	…	64.1	…
7	3s	…	…	…	…	…	0.1488	1.661	0.2045	…	…	2.09	…	9.18	…
8	4s	…	…	…	…	…	0.1488	1.661	0.2045	…	…	2.09	…	9.18	…
9	5s	…	…	…	…	…	0.1488	1.509	0.1268			7.26	…	32.2	…
10	6s	…	…	…	…	…	0.1488	1.659	0.2014	…	…	1.96	…	7.52	…

Source: Ref 4

The effective strain and stress factor state were established by two methods. In the first method measurements were made of η and ξ from the distortion of the grid cut on specimens; based on these data, k and g_{iz} were determined (Ref 38). In the second method η was established on the basis of specimen diameters measured before and after deformation. With the known η and m, as determined by the first method (Ref 38) (m being dependent on friction), determinations were made of k and g_{iz} (Ref 4). In this test η and ξ were determined from the equations:

$$\eta = \log \frac{d_1}{d_0} \quad \text{(Eq 19)}$$

$$\xi = \log \frac{b_0}{b_1} \quad \text{(Eq 20)}$$

where d_0 and d_1 are the diameter of specimen at maximum barreling, before and after the test, respectively, and b_0 and b_1 are the height of grid mesh before and after test, at the spot of fracture.

On the surface of some specimens there was an orthogonal grid with the mesh of 1 mm. Specimens designated with *s* had the grid and those designated with *b* had no grid. Tables 2 to 5 list the results of the upending test (Ref 4).

5. Conclusions

Six points of the deformation curve for K18 steel were obtained. Final results (values of stress state factor and effective strain) are given in Table 6. Based on these data the curve of deformability for K18 steel has been plotted in Fig. 2. This curve is the image of the decreasing function. As the stress factor increases, the degree of deformation (effective strain) decreases, which is necessary to cause fracture of the material. Thus, there is a decrease in plasticity of the material. The well-known fact that plasticity characterizes not only the material but also the state of stress has been confirmed.

It can be seen from Fig. 2 that with the stress factor $k = 2$, the plasticity of material is very low. Hence it can be concluded that there exists a certain boundary value of k, at which the degree of deformation at fracture is 0. With such a stress state the steel of K18 grade will behave as a brittle material. Considering the data listed in Table 6, it can be said that the tensile test on notched specimens and the upending test on cylindrical specimens did not allow (one case excepted) a stress state for which the stress factor would be negative to be obtained. From the analysis made in section 3, this is not necessary for the majority of working processes.

Boundary deformability was widely investigated in Ref 14 to 22. Curves of deformability were determined by using circumferentially notched tensile specimens. Plane strain notched tensile specimens were used occasionally. Torsion tests and compression tests were not used. Industrial processes such as tube drawing and rolling have compressive stresses, so use for modeling only tensile tests does not seem proper. Results of this investigation were used to study mechanism of failure before cracks occurred in plane-strain conditions (Ref 21) and in notched bar in bending (Ref 15), which seems to have little practical meaning. The theory of boundary deformability can be used for practical purposes (Ref 1, 2, 7, 40).

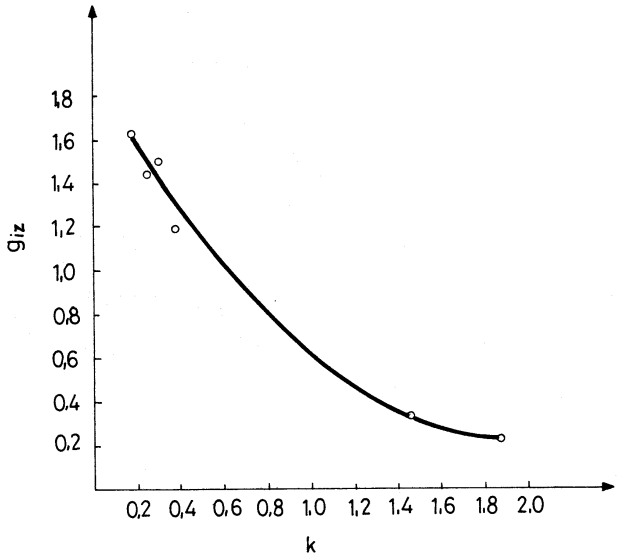

Fig. 2 Deformability curve for K18 steel (Ref 4, 5)

Table 6 State of stress factor and effective strain at fracture

k	g_{iz}
0.1873	1.627
0.252	1.455
0.3034	1.509
0.385	1.1995
1.464	0.325
1.887	0.229

Smooth and notched tensile specimens were used to determine deformability curves in research (Ref 24-26). The problem is that this part of the deformability curve is not essential from a practical point of view.

References

1. W.L. Kolmogorow, Utilization of Reserve of Plasticity of Metals during Production of Drawing Tubes, *Swierdlowskoje Kniznoje Izdatielstwo,* 1966
2. W.L. Kolmogorow, Stresses, Strains, Fracture, *Izd. Mietallurgija,* Moskwa, 1970
3. K. Takase, On the Creation of Microcrack by Plastic Deformation of Medium Carbon Steel, *Proceedings of the International Conference on the Strength of Metals and Alloys* (Tokyo), 1967
4. J. Pospiech, *Prace IH,* Vol 24 (No. 4), 1972, p 237-245
5. J. Pospiech, STRUCMAT 87: International Conference on Computational Methods for Predicting Material Processing Defects (Cachan, France), *Studies in Applied Mechanics 15, Computational Methods for Predicting Material Processing Defects,* M. Predeleanu, Ed., Elsevier, 1987, p 289-294
6. J. Pospiech, *Prace IH,* Vol 25 (No. 5), 1973, p 205-208
7. J. Pospiech, *Prace IH,* Vol 26 (No. 3), 1974, p 159-164
8. J. Pospiech, *J. Mech. Work. Technol.,* Vol 10 (No. 3), 1984, p 325-347
9. J. Pospiech, *J. Mech. Work. Technol.,* Vol 13 (No. 1), 1986, p 5-22
10. J. Pospiech, *J. Mech. Work. Technol.,* Vol 12 (No. 1), 1985, p 93-114

11. J. Pospiech, *J. Mater. Eng. Perform.*, Vol 4 (No. 1), Feb 1995, p 82-89
12. J. Pospiech, *Steel Times*, Vol 223 (No. 9), 1995, p 354, 356
13. J. Pospiech, R. Sulkowski, and H. Szwej, *Steel Times*, Vol 224 (No. 4), 1996, p 145-146
14. J.W. Hancock and A.C. Mackenzie, *J. Mech. Phys. Solids*, Vol 24 (No. 2/3), 1976, p 147-169
15. A.C. Mackenzie, J.W. Hancock, and D.K. Brown, *Eng. Fracture Mech.*, Vol 9 (No. 1), 1977, p 167-188
16. J.W. Hancock and A.C. Mackenzie, *J. Mech. Phys. Solids*, Vol 24 (No. 2/3), 1976, p 147-169
17. J.W. Hancock and D.K. Brown, *J. Mech. Phys. Solids*, Vol 31 (No. 1), 1983, p 1-24
18. R.D. Thomson and J.W. Hancock, *Int. J. Fracture*, Vol 24, 1984, p 209-228
19. R.D. Thomson and J.W. Hancock, *Int. J. Fracture*, Vol 26, 1984, p 99-112
20. J.W. Hancock and R.D. Thomson, *Mater. Sci. Technol.*, Vol 1 (No. 9), 1985, p 684-690
21. J.W. Hancock and M.J. Cowling, *Metal Sci.*, Vol 14 (No. 8/9), 1980, p 293-304
22. J. Orr and D.K. Brown, *Eng. Fracture Mech.*, Vol 6 (No. 2), 1974, p 261-274
23. J.R. Rice and D.M. Tracey, *J. Mech. Phys. Solids*, Vol 17, 1969, p 201-217
24. E. El-Magd, *Steel Res.*, Vol 68 (No. 2), 1997, p 67-71
25. D. Holland, X. Kong, N. Schlüter, and W. Dahl, *Steel Res.*, Vol 63 (No. 8), 1992, p 361-367
26. D. Holland, A. Halim, and W. Dahl, *Steel Res.*, Vol 61 (No. 10), 1990, p 504-506
27. P.F. Thomason, *Mem. Sc. Rev. Metall.*, Vol 20 (No. 5), 1983, p 233-239
28. M. Vater and A. Lienhart, *Bänder Bleche Rohre*, Vol 13 (No. 8), 1972, p 387-395
29. H. Schiller, *Neue Hütte*, Vol 17 (No. 7), 1972, p 426-431
30. M. Schneider, *Drawing of Steels*, Katowice, 1951
31. I.L. Pierlin, Theory of Drawing, Gosudarstwiennoje Nauczno-Tiechniczeskoje Izdatielstwo Literatury po Czornoj i Cwietnoj Mietallurgii, Moskwa, 1957
32. G. Arkulis, Plastic Deformations of Metals, *Izd. Mietallurgia*, Moskwa, 1964
33. Poradnik Techniczny. Mechanik. Tom III. Part 1-2, *Metal Forming Handbook*, PWT, Warszawa, 1954
34. Z. Wusatowski, *Fundamentals of Rolling*, Katowice, 1960
35. Z. Wusatowski, *Fundamentals of Rolling*, W. Slask, Ed., Katowice, 1969
36. A.I. Celikow, Rolling Mills, *Mietallurgizdat*, Moskwa, 1964
37. W. Gorecki and K. Mniszek, "Research Report of IMZ," No. N-975, Research Institute of Ferrous Metallurgy, unpublished
38. G.A. Smirnow-Alajew, Resistance of Materials Against Metal Forming, Leningrad, Maszgizd, Moskwa, 1961
39. J. Wójcikowki et al., *Laboratory of Technology of Machines*, Part 1, Politechnika Slaska, Gliwice, 1967
40. K. Takase and Y. Kurita, Proceedings ICSTIS, *Suppl. Trans. Iron Steel Inst. Jpn.*, Vol 11, 1971, p 862-867